Geotech Geol Eng (2022) 40:5725–5738
https://doi.org/10.1007/s10706-022-02244-0

ORIGINAL PAPER

Resonant Column Tests on Mixtures of Different Sands with Coarse Tyre Rubber Chips

Gerard Banzibaganye · Christos Vrettos

Received: 27 January 2022 / Accepted: 11 July 2022 / Published online: 20 August 2022
© The Author(s) 2022

Abstract The dynamic behaviour of unsaturated sand rubber chips mixtures at various gravimetric contents is evaluated through an experimental study comprising resonant column tests in a fixed-free device. Chips were irregularly shaped with dimensions ranging from 5 to 14 mm. Three types of sand with different gradation have been considered. Relative density amounted to 0.5 for all specimens. Due to the large size of the chips, the diameter of the specimens had to be equal to 100 mm, which in turn required a re-calibration of the device assuming a frequency-dependent drive head inertia. The effects of confining stress, rubber chips content, and sand gradation on shear modulus and damping ratio are determined over wide ranges of the shear strain. At small strains, as known for sands, increasing the confining stress stiffens the mixtures. Increasing the rubber chips content reduces significantly the shear modulus and increases the damping ratio. At higher strains, increasing the confining stress or the rubber content flattens the reduction of the shear modulus with strain. Damping at high strains does not show any appreciable dependence on rubber content. Unloading–reloading sequences are used to assess shear modulus degradation and threshold strains. Finally, design equations are derived from the test results to predict the dynamic response of the composite material.

Keywords Shredded tyre rubber chips · Sand and rubber mixtures · Resonant column test · Shear modulus · Damping

G. Banzibaganye · C. Vrettos (✉)
Division of Soil Mechanics and Foundation Engineering, Technical University of Kaiserslautern, 67663, Germany, Kaiserslautern

G. Banzibaganye
Department of Civil, Environmental and Geomatics Engineering, University of Rwanda, Rwanda, Kigali
e-mail: vrettos@rhrk.uni-kl.de

1 Introduction

Soils subjected to vibrations induced by earthquakes, traffic loads, wind turbines, etc. cause many geotechnical engineering problems. A thorough understanding of these problems is based on the evaluation of the dynamic response, i.e. shear modulus and damping, prior to design and construction. The encountered challenges can be addressed through various techniques of ground improvement, such as soil reinforcement employing tyre shreds, chips or rubber granulates. This is an innovative technology of the ground improvement following the damping waste tyre bans in different countries. In geotechnical engineering, the soil rubber composite material found its application in various projects such as highway embankment fills, retaining walls and bridge abutment backfills, seismic isolation for the foundation of different structures and so forth. This geomaterial

possesses excellent geotechnical properties in terms of drainage characteristics, shear strength, resistance to liquefaction and damping capability.

Literature includes a bank of data on the application of this modern technology. With respect to static behaviour due to static loading one may mention the work by Foose et al. (1996), Zornberg et al. (2004), Becker and Vrettos (2011). In respect of cyclic behaviour evaluated using cyclic simple shear and cyclic triaxial apparatuses, one may acknowledge the works by Nakhaei et al. (2012), Kaneko et al. (2013), Mashiri et al. (2016), Li et al. (2016), Madhusudhan et al. (2018), Bahadori and Farzalizadeh (2018), Banzibaganye et al. (2019), Hazarika et al. (2020), Amuthan et al. (2020), Das and Bhowmik (2020), Madhusudhan et al. (2020), Rios et al. (2021) Banzibaganye and Vrettos (2022). The dynamic behaviour of sand rubber mixtures was evaluated in few studies using a resonant column device. One can mention the works by Feng and Sutter (2000), Senetakis et al. (2011) (2012), Anastasiadis et al. (2012), Ehsani et al. (2015), Pistolas et al. (2018). Compared to pure sands, the results from these studies showed an improvement of damping ratio associated with a decrease in shear modulus. Large scale tests showed the effectiveness as a means of geotechnical seismic isolation (Pitilakis et al. 2021).

In the studies conducted hitherto on sand rubber mixtures using the resonant column device, the particle size of the rubber was limited to a maximum 6 mm in diameter, the material being classified as fine rubber chips or coarse rubber granulate (Madhusudhan et al. 2020). Studies by Hong et al. (2015) and Shariatmadari et al. (2018) using triaxial equipment showed that the granulated rubber materials reduce the static shear strength and increase the liquefaction resistance of sand. Amuthan et al. (2020) investigated sand mixed with granulated rubber smaller than 2 mm with various rubber contents and reported contradictory findings. A decrease in shear strength and liquefaction resistance of sands mixed with fine rubber material could be discouraging for the use of this composite geo-material as a fill or backfill in civil/geotechnical engineering applications. In previous studies by the authors (Banzibaganye et al., 2019; Banzibaganye and Vrettos, 2022) sand was mixed with irregular, coarse rubber chips ranging in size between 4 and 14 mm. The results showed a significant improvement in shear strength for all rubber contents, as well as an increase of cyclic resistance for rubber contents larger than 10%.

In the studies mentioned above, that mostly deal with rubber granulate or small-size chips, resonant column testing was performed on specimens with a diameter not exceeding 70 mm, which is however small when the rubber chips become too large. Since in the present investigation irregular chips with dimensions up to 14 mm are considered, a specimen of 100 mm in diameter was selected in order to fulfil the common requirement of a diameter at least six times the largest particle size, cf. ASTM D4015-15e1 (2015). Small-strain and intermediate strain values of shear modulus and damping ratio of the composite material have been determined using standard techniques. Moreover, the threshold strain associated with the onset of a shear modulus degradation was assessed by means of unloading–reloading paths at distinct strain levels. Common functional relationships for shear modulus and damping ratio are extended to account for the effects of the rubber chips content on the dynamic response of the composite material.

2 Material and Testing

2.1 Material

Three types of clean sand S2, S3 and S4 were used in this study, with particle size distribution as shown in Fig. 1. They are classified as uniform medium sand, uniform coarse sand, and poorly graded sand, respectively. Their properties are summarized in Table 1 and include specific gravity G_s, mean grain size d_{50},

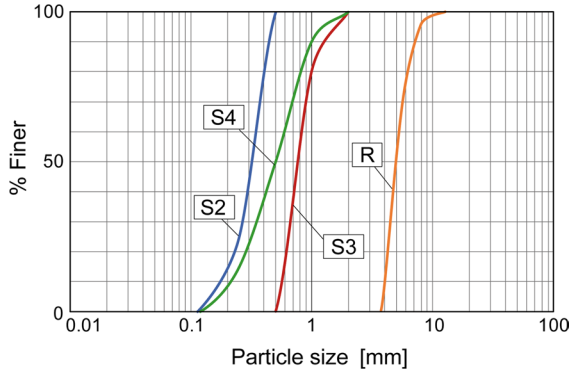

Fig. 1 Particle size distribution for the different sands (S2, S3, S4) and the rubber chips (R)

Table 1 Properties of the sands used

Description	S2	S3	S4
G_s	2.65	2.65	2.65
d_{50} [mm]	0.32	0.77	0.5
C_u [-]	1.7	1.5	2.7
C_c [-]	1	0.9	1
$\rho_{d,max}$ [g/cm^3]	1.591	1.663	1.798
$\rho_{d,min}$ [g/cm^3]	1.388	1.466	1.466
e_{min} [-]	0.665	0.594	0.474
e_{max} [-]	0.909	0.807	0.807

uniformity coefficient C_u, coefficient of curvature C_c, minimum and maximum values of dry density and void ratio, $\rho_{d,min}$, $\rho_{d,max}$, and e_{min} and e_{max}, respectively. Furthermore, standard triaxial compression tests according to DIN EN ISO 17,892–9 were conducted at specific values of initial void ratio e_0. The derived shear strength parameters at peak, i.e. angle of internal friction φ' and cohesion intercept c' are: for S2/S3/S4 at $e_0 = 0.748/0.666/ 0.588$: φ'[°]; c' [kPa] = 37.5;9.5/35.5;8,7/27.0;10.3.

Shredded tyre material, free of steel, wires and fibers, was collected from a local tyre recycling company. The desired particle size distribution, displayed in Fig. 1, was obtained by appropriate sieving. Specific gravity determined in the laboratory varied between 0.98 and 1.1, and an average of 1.05 was used. Proctor density in dry condition amounted to 0.64 g/cm^3. Hardness was determined using the Shore durometer scale (Shore A). The results from fifteen smoothed surface rubber pieces tested showed values between 64 and 67 with an average of 66. This indicates that the rubber chips are of the same hardness, and can be classified accordingly as medium hard. Shear strength parameters derived from triaxial tests at dry density $\rho_d = 0.504$ g/cm^3 for isotropic confining stress of 50, 100 and 200 kPa were $\varphi' = 13.2°$ and $c' = 20.3$ kPa. The respective values determined at the same density by means of a large direct shear box (30 × 30 cm) according to DIN EN ISO 17892–10 were $\varphi' = 25.2°$ and $c' = 7.9$ kPa.

The mixtures were prepared in dependence on the target rubber chips content χ which amounted to 0, 10, 20 and 30% by dry mass. The mixtures were named according to the sand matrix S2RM, S3RM, or S4RM. A photograph of a typical mixture is given in Fig. 2. Minimum and maximum densities of the composite materials were determined according to the standards for cohesionless soils, and are given in Table 2. The segregation of the individual particles was likely to occur for chips contents over 20%. To prevent this, each specimen was prepared by placing the material in successive sublayers of known mass for each of the two constituents.

2.2 Equipment, Specimen Preparation and Testing

A Stokoe-type resonant column device with a fixed-free configuration, supplied by GDS, UK was utilized, cf. Figure 3. It was enhanced and calibrated accordingly to accommodate different specimen sizes. The testing principles specified in the pertinent standard ASTM D4015-15e (2015) for torsional excitation have been considered. The standard procedure based on sweeping the frequency around resonance was applied in the tests. The damping ratio was determined by the free-vibration decay method. For complete operating details, the reader is referred to the handbook provided by the manufacturer (GDS 2015).The use of large specimens, with dimensions of 100 mm in diameter and 200 mm in height, required an adaption of the calibration method assuming a frequency-dependent inertia of the drive head. The equivalent homogeneous strain in the specimen is set equal to 80% of the strain at the perimeter of the specimen's top end as inferred from the measurement. This assumption is important when comparing with results from other studies. Details for the calibration and the data reduction are described by Vrettos and

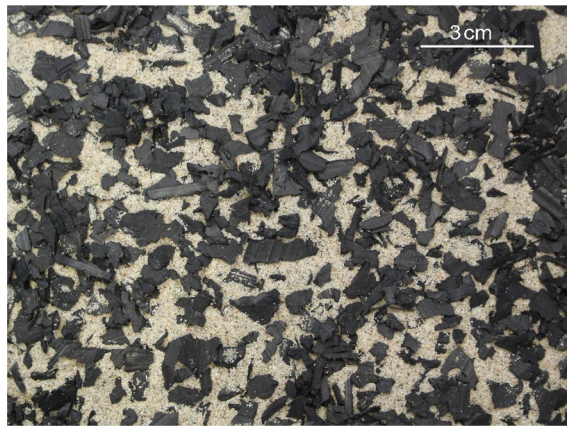

Fig. 2 Medium sand S2 mixed with rubber chips at 20% chips

Table 2 Specimen composition, densities, cell pressures, and small strain values for shear modulus and damping ratio measured in the multi-stage resonant column tests

Soil	χ [%]	ρ_d [g/cm^3]	$\rho_{d,\min}/\rho_{d,\max}$ [g/cm^3]	σ'_0 [kPa]	$G_{\max}$ [MPa]	$D_{\min}$ [%]
S2	0	1.484	1.388/1.588	50	63.2	0.37
				100	82.1	0.36
				200	117.8	0.29
				300	140.3	0.23
				400	160.9	0.35
	10	1.393	1.292/1.514	50	38.2	0.76
				100	51.4	0.70
				200	70.1	0.63
				300	85.2	0.69
	20	1.287	1.191/1.401	50	19.4	1.08
				100	27.7	1.10
				200	39.5	0.96
				300	48.0	0.98
	30	1.171	1.076/1.285	50	10.2	1.88
				100	15.0	1.82
				200	22.3	1.80
				300	28.3	1.80
S3	0	1.558	1.466/1.663	50	80.3	0.40
				100	111.7	0.34
				200	153.4	0.39
				300	183.8	0.37
				400	213.6	0.38
	10	1.365	1.274/1.474	50	28.7	0.87
				100	40.3	0.83
				200	58.0	0.79
				300	69.2	0.68
	20	1.228	1.136/1.339	50	14.0	1.6
				100	19.0	1.5
				200	29.3	1.4
	30	1.095	0.983/1.181	50	5.3	2.39
				100	8.3	2.35
				200	14.7	2.18

Table 2 (continued)

Soil	χ [%]	ρ_d [g/cm^3]	$\rho_{d,\min}/\rho_{d,\max}$ [g/cm^3]	σ'_0 [kPa]	$G_{\max}$ [MPa]	$D_{\min}$ [%]
S4	0	1.615	1.466/1.798	50	72.2	0.38
				100	97.7	0.38
				200	138.6	0.43
				300	170.0	0.39
				400	189.0	0.38
	10	1.436	1.320/1.575	50	33.7	0.86
				100	44.2	0.79
				200	64.6	0.71
				300	77.8	0.66
	20	1.307	1.228/1.397	50	15.1	1.08
				100	22.5	1.01
				200	33.5	0.96
				300	41.4	0.98
	30	1.189	1.106/1.287	50	9.0	1.56
				100	13.0	1.52
				200	20.6	1.35
				300	25.7	1.28

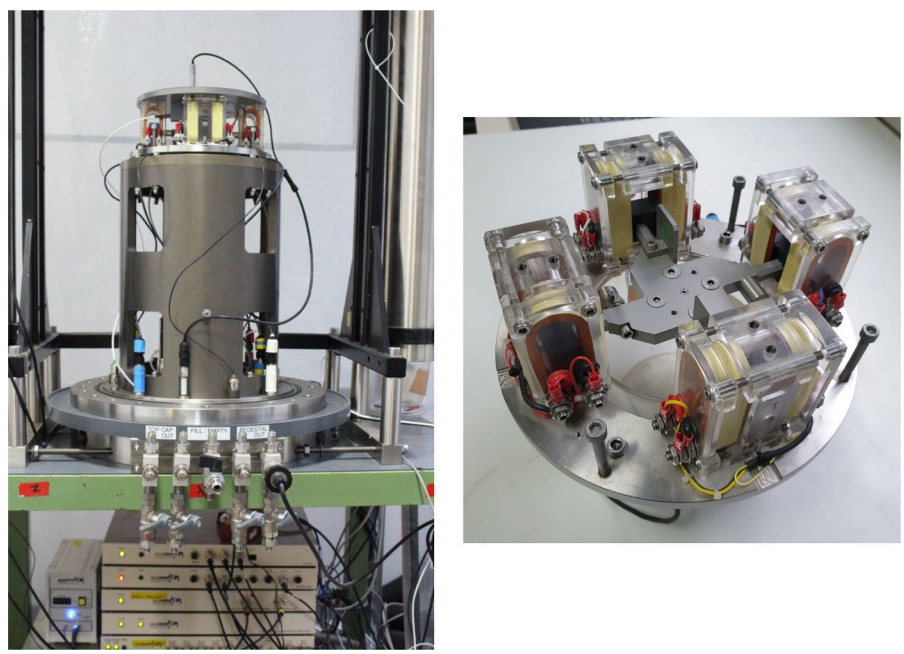

Fig. 3 Resonant column device and drive head

Banzibaganye (2022). An isotropic confining stress was applied through control of the cell pressure.

The specimen preparation technique is described by Banzbaganye and Vrettos (2022). Wet tamping with a residual water content of 5% was applied to prevent segregation of particles. The total target mass of the sample was divided into five equal portions, each transferred into a sample preparation mould, and compacted in order to achieve a sublayer thickness of 40 mm (total height 200 mm). A small vacuum of approximatively 10 kPa was applied to ensure the stability of the specimen during the removal of the mould as well as the connection to the drive plate. The examined material included a rubber chips content of up to 30%. At higher rubber chips contents, some of the specimen experienced even under this small vacuum a non-negligible compression, which required an adjustment of the level of the magnet coils in the driving system. Figure 4 shows a test specimen at a rubber chips content of 30%. The particular specimen has been frozen for two hours on the base pedestal using dry ice. It can be seen that wet tamping yields a uniform mixture with random positions and orientations of the chips.

The target relative density I_D for the sands and all mixed samples was set equal to 0.5. Minimum and maximal densities determined in accordance with DIN 18126:1996–11 are given in Table 2. All test data are summarized in Table 2 including the dry density of the composite material ρ_d and the effective confining stress (cell pressure) σ'_0.

Fig. 4 Test specimen stabilized by dry-ice freezing for the sake of visualization (Banzibaganye and Vrettos, 2022)

The resonant column investigations comprised multi-stage and single-stage tests. In the former, a low amplitude test sequence, with the soil remaining within the elastic limit, is first conducted by stepwise increasing the effective confining stress up to an upper value. At each confining stress level (stage), the shear modulus G and the damping ratio D are measured for several strain amplitudes within the elastic response range. These values are denoted by $G_{\max}$ and $D_{\min}$. Loading is interrupted as soon as the modulus exhibits a decay of approximately 3%. The subsequent unloading to a considerably reduced amplitude (small strains) with measurement of shear modulus provides a control that no degradation occurred. Cell pressure is then increased to the next higher level. Testing started a confining stress equal to 50 kPa and went up to 400 kPa for the sands and 300 kPa for the sand-rubber mixtures, respectively. At each particular stage the specimen was allowed to consolidate for a period of approximately 40 min in order to reach an equilibrium. For intermediate and high strain testing, a fresh specimen was tested at each distinct confining stress level. Cycles of unloading–reloading were also applied in order to assess possible modulus degradation. The first unloading was performed at the beginning of the modulus decay curve and then at $G/G_{\max} = 0.90$, 0.85 and 0.80.

3 Results and Discussion

3.1 Small Strain Response

Values for the small strain shear modulus $G_{\max}$ and damping ratio $D_{\min}$ for the sands S2, S3 and S4 mixed with rubber chips at different contents as derived from the multi-stage tests are given in Table 2. The respective shear strain amplitudes γ were in the order of 10^{-4}% for both the sands and the composite materials. As shown by the data, $G_{\max}$ increases with increasing confining stress and decreases with increasing rubber chips content. The results for $D_{\min}$ exhibit a weak dependence on confining stress, but a significant increase with the rubber chips content.

For pure rubber chips, a shear modulus of around 1.2 MPa and a D_{min} value of around 6% are reported in the literature by Anastasiadis et al. (2012). Own results derived from cyclic triaxial tests on rubber chips are of similar magnitude. The increase of shear modulus with effective confining stress is a well-known property of granular materials. The trends observed when the rubber content increases can be attributed to decreased density, increased elasticity and compressibility due to the presence of rubber in the mixtures. The experimental results further suggest that sand S3 has the highest G_{max} with no rubber but drops to lower values than the other sands with rubber addition, and the reverse is observed for sand S2. Evidently, the coarse rubber chips used herein interact better with sand S2 than with the coarser sand S3.

Figure 5 displays G_{max} versus χ for various mixtures at a confining stress $\sigma'_0 = 100$ kPa, which is typical for near-surface engineering applications. It includes the respective G_{max} values reported by Bernal-Sanchez et al. (2019) for coarse sand with $d_{50} = 0.85$ mm, $C_u = 1.27$ mixed with rubber granulate ($d_{50} = 1.3$ mm), which are in good agreement with those obtained herein. It can be seen that at higher values of rubber content $\chi \geq 20\%$, the data points for all sands exhibit only minor differences.

Based on the data in Table 3 an equation for the dependence of G_{max} on the confining stress σ'_0 is derived. A simple power-law can be employed with a fixed exponent equal to 0.5, which is widely accepted in soil dynamics. Curve-fitting by adopting Eq. (1)

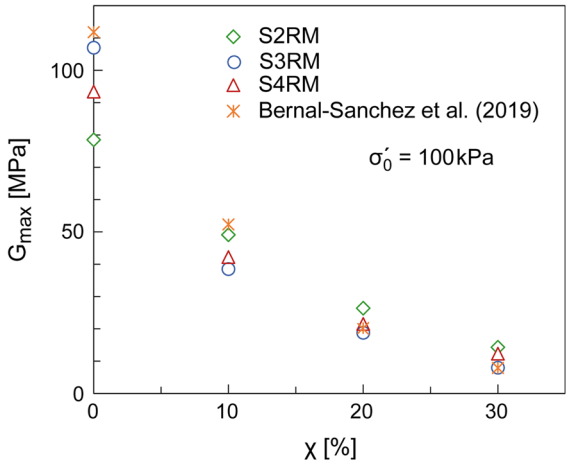

Fig. 5 Variation of small strain shear modulus with rubber chips content for various mixtures at 100 kPa

Table 3 Constants in Eqs. (1) and (2) for different types of sand rubber mixture at $I_D = 0.5$

Material	A_G	d_G	A_D	d_D
Sand S2 and S2RM	820	0.0527	0.30	0.174
Sand S3 and S3RM	1070	0.0895	0.36	0.182
Sand S4 and S4RM	960	0.0700	0.37	0.135

yields the numerical values for the parameters given in Table 3 for the different sand rubber mixtures.

$$G_{max} = A_G \cdot \exp\left(-d_G \cdot \chi\right) \cdot \left(\sigma'_0/p_a\right)^{0.5} \cdot p_a \quad (1)$$

where p_a is the atmospheric pressure (100 kPa); $0 \leq \chi \leq 30\%$; $50 \leq \sigma'_0 \leq 300$ kPa.

A relationship is also derived for the small strain damping ratio D_{min}, merely in dependence on the rubber content as the variation with confining stress is not significant and with no clear trend. Curve-fitting over $0 \leq \chi \leq 30\%$ and $50 \leq \sigma'_0 \leq 300$ kPa yields Eq. (2) with the constants given in Table 3.

$$D_{min} = A_D \cdot \exp\left(-d_D \cdot \chi^{0.68}\right) \quad (2)$$

Figure 6 compares the measured values G_{max} and D_{min} with the predictive Eqs. (1) and (2) at 100 kPa, manifesting the good accuracy of the proposed design equations. The same holds for the other confining stresses investigated herein. It can be seen that A_G and d_G increase with the median grain size of the sand.

Equations (1) and (2) may be used to approximately predict the small strain response at higher rubber contents that could not be measured in the tests due to the high compressibility of the mixtures. For $\chi = 0.5$ at 100 kPa, for example, the predicted G_{max} for S2RM equals 5.88 MPa compared to 82 MPa for pure sand, which is a dramatic reduction in stiffness. For S4RM, G_{max} reduces to 2.05 MPa compared to 96 MPa for pure sand, and for S3RM $G_{max} = 1.21$ MPa instead of 107 MPa. Consequently, the particular material is expected to behave almost similar to pure rubber already at this rubber content.

3.2 Intermediate Strain Response

Single stage tests at different confining stresses were conducted for this purpose. The small strain values were almost identical to those derived from the multi-stage tests. First, results for pure sand are presented.

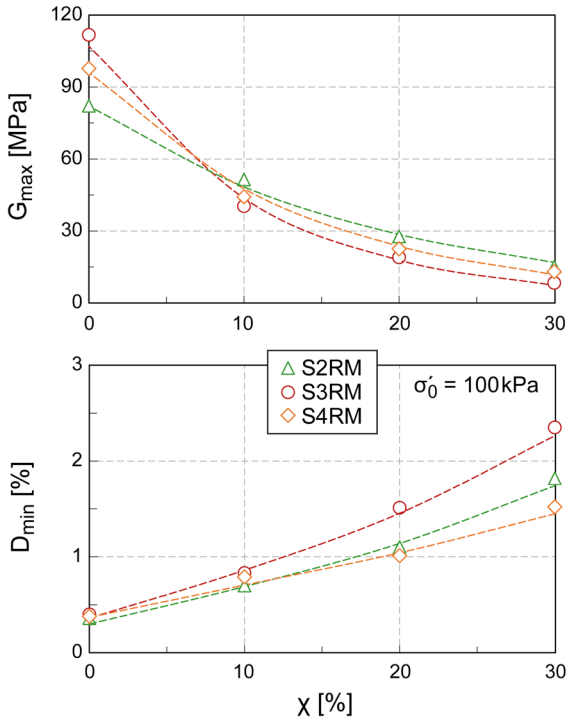

Fig. 6 Small strain shear modulus and damping ratio vs. rubber chips content for different mixtures at confining stress of 100 kPa. The dashed lines represent Eqs. (1) and (2)

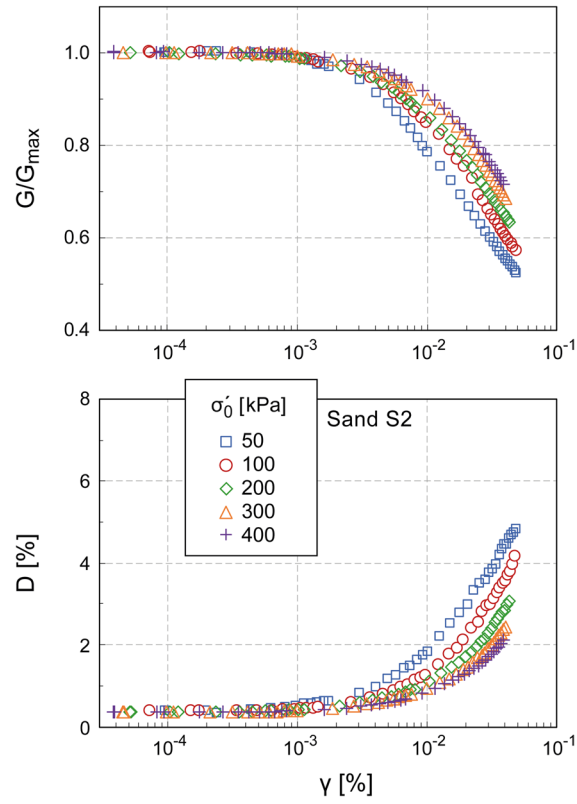

Fig. 7 Shear modulus reduction G/G_{max} and damping ratio D vs. shear strain at different confining stresses for pure sand S2

Figure 7 depicts the shear modulus reduction and damping ratio increase with shear strain amplitude for sand S2. Similar curves were obtained for sands S3 and S4 and can be found in Banzibaganye (2022). Due to the large specimen size and inertia, the maximum attainable strain level was limited in the tests with the particular device. S3RM at $\chi = 30\%$ was soft and the tests ended at lower intermediate strain amplitudes. During the tests on S3RM at $\chi = 20\%$ and 30% under confining stress of 300 kPa, contact between the magnets and the bottom part of the coils occurred, which led to the cancellation of the tests. The results confirm the well-known property that the shear modulus reduction becomes stronger as the confining stress decreases whereas the damping increases (Vrettos and Banzibaganye, 2022).

The results for the various sand-rubber mixtures confirmed these trends: higher confining stress increases the range over which shear modulus and damping ratio remain within the elastic domain with negligible reduction of the small strain values. Increasing the rubber content decreases G and increases G/G_{max} and D. The same observations are reported by Anastasiadis et al. (2012), Senetakis et al. (2012), Ehsani et al. (2015) and Pistolas et al. (2018).

Typical results for the strain dependency of G/G_{max} and D in sand rubber mixtures are displayed in Fig. 8 and Fig. 9 for confining stress of 100 kPa. The influence of confining stress on the behaviour of the mixtures is exemplarily shown in Fig. 10 and Fig. 11 for S2RM. These curves are part of the complete experimental data set that is documented in Banzibaganye (2022). It covers confining stresses from 50 to 300 kPa and rubber chips contents equal to 0, 10, 20 and 30%. The trends observed in these figures are valid also for the other sands and their mixtures. A salient feature is the extended range of linear behaviour, i.e. the shifting of the G/G_{max}–γ curve to the top right of the plot, as more rubber chips are added to the sand, cf. Figure 9 for sand S4. This is important with regard to the seismic site response when the ground is improved by adding rubber chips to the sand.

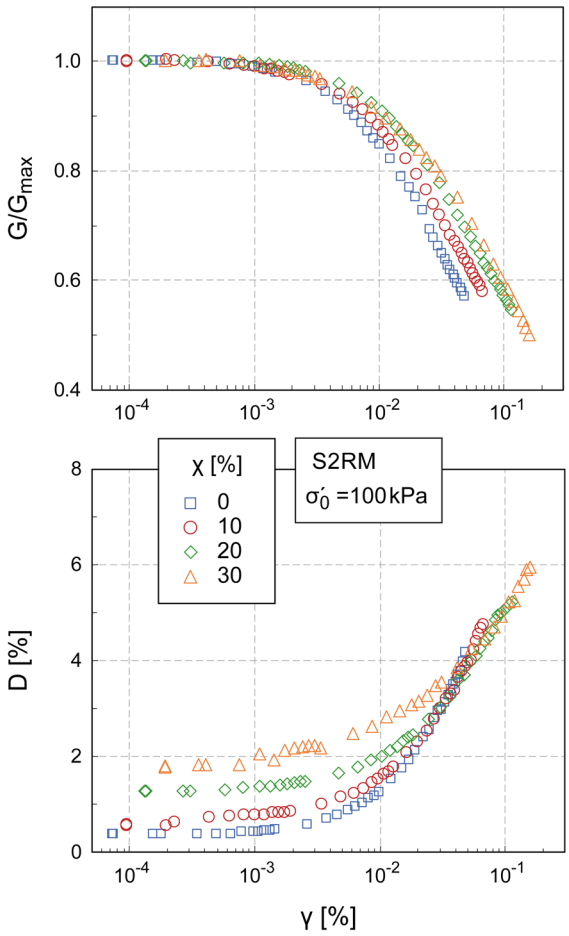

Fig. 8 Effect of rubber content on shear modulus reduction and damping ratio vs. shear strain for mixture S2RM at confining stress of 100 kPa

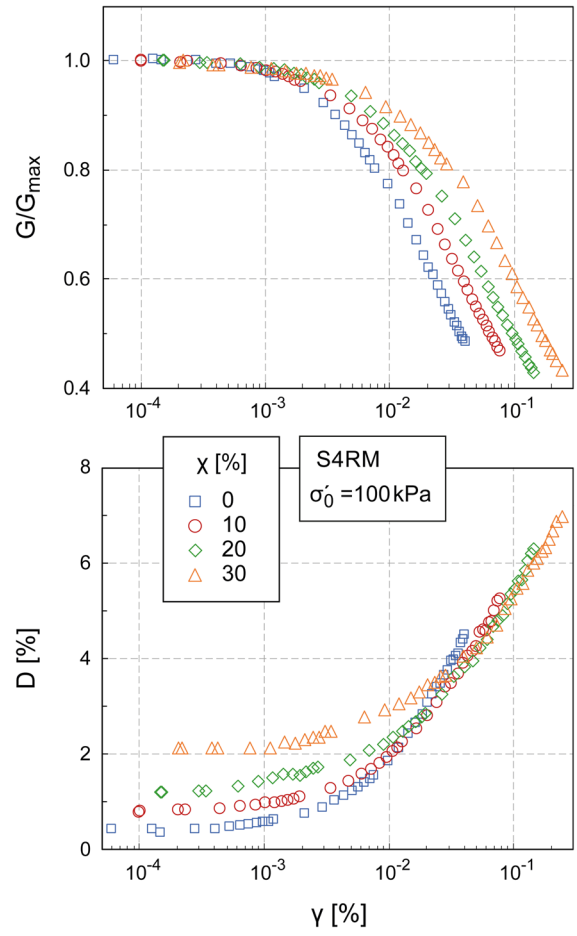

Fig. 9 Effect of rubber content on shear modulus reduction and damping ratio vs. shear strain for mixture S4RM at confining stress of 100 kPa

During vibration, particles in pure sand may develop hysteretic damping through friction between them, with limited or no energy dissipation through particle deformation. However, when mixed with rubber, damping is induced not only by the friction between sand and rubber particles but also by the deformation of the rubber particles, cf. Fonseca et al. (2019). As a result, increasing the rubber content in the mixtures leads to an increase of the damping ratio as well.

The shear modulus reduction curves obtained from the different sand rubber mixtures in the tests can be approximated by means of a hyperbolic law as suggested among others by Vrettos and Savidis (1999) taking into account the rubber chips content and the confining stress:

$$\frac{G}{G_{\max}} = \frac{1}{1 + g_1 \cdot \gamma^{\alpha_1}} \tag{3}$$

The parameter g_1 is a function of the rubber content and the effective confining stress, whereas α_1 is fixed to $\alpha_1 = 0.9$. Using linear regression, the following equation is derived for all mixtures considered:

$$g_1 = A_q \cdot \exp(d_q \cdot \chi) \left(\frac{\sigma_0'}{p_a} \right)^{-0.3} \tag{4}$$

for $0 \le \chi \le 30\%$ and $50 \le \sigma_0' \le 400$ kPa. Values of the constants A_q and d_q are given in Table 4 and cover also pure sand. The quality of the approximation is exemplarily shown in Fig. 12 for S4RM at 100 kPa,

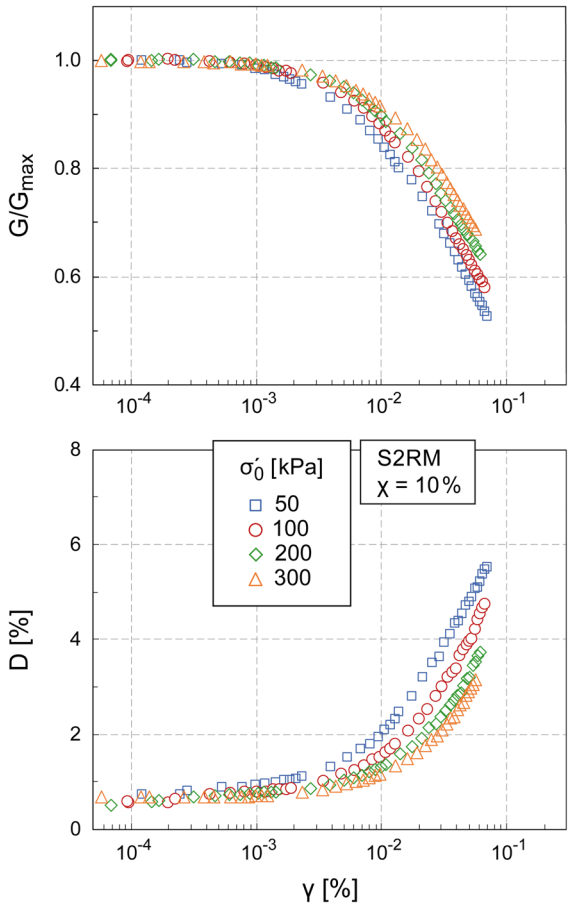

Fig. 10 Shear modulus reduction and damping ratio versus shear strain at different confining stresses for sands S2RM at a rubber content of 10%

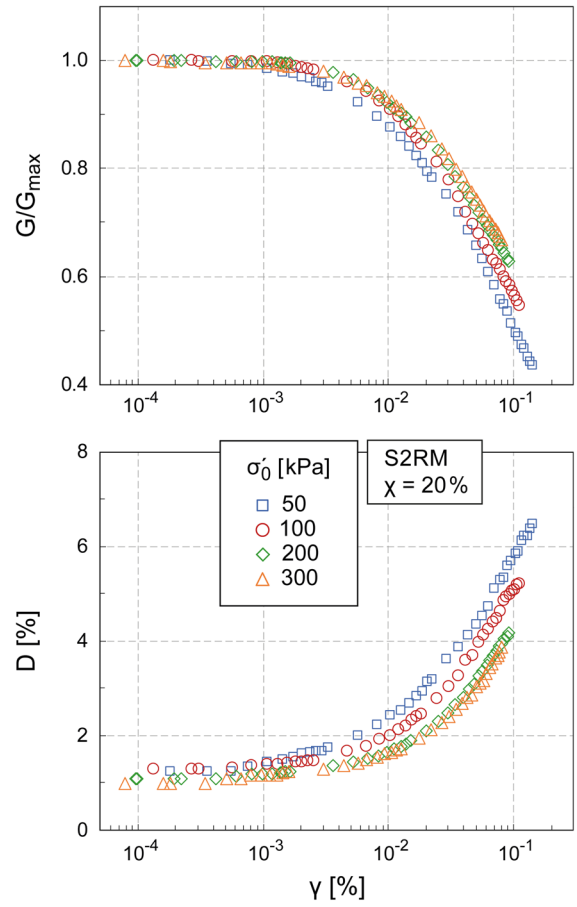

Fig. 11 Shear modulus reduction and damping ratio versus shear strain at different confining stresses for sands S2RM at a rubber content of 20%

Table 4 Constants in Eq. (4)

Material	A_q	d_q
Sand S2 and S2RM	11.53	−0.026
Sand S3 and S3RM	12.29	−0.058
Sand S4 and S4RM	18.82	−0.042

whereby the curves have been extended to very high strains to visualize the expected behaviour of the mixtures.

3.3 Shear Modulus Degradation

In order to assess the strain-dependent degradation upon unloading and the threshold shear strain

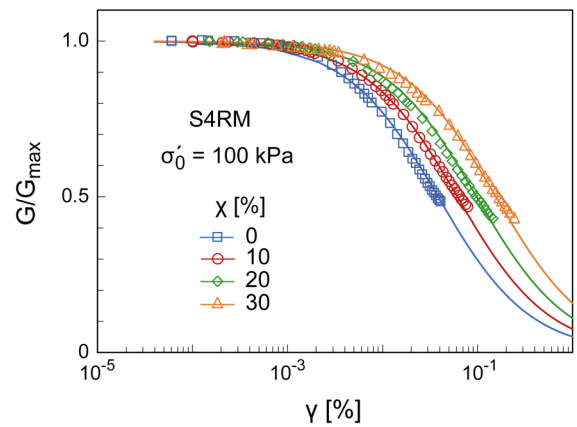

Fig. 12 Approximation of the shear modulus reduction for mixture S4RM for different rubber chips contents at confining stress of 100 kPa. The symbols are for the test data, the solid lines for Eq. (3) in conjunction with Eq. (4)

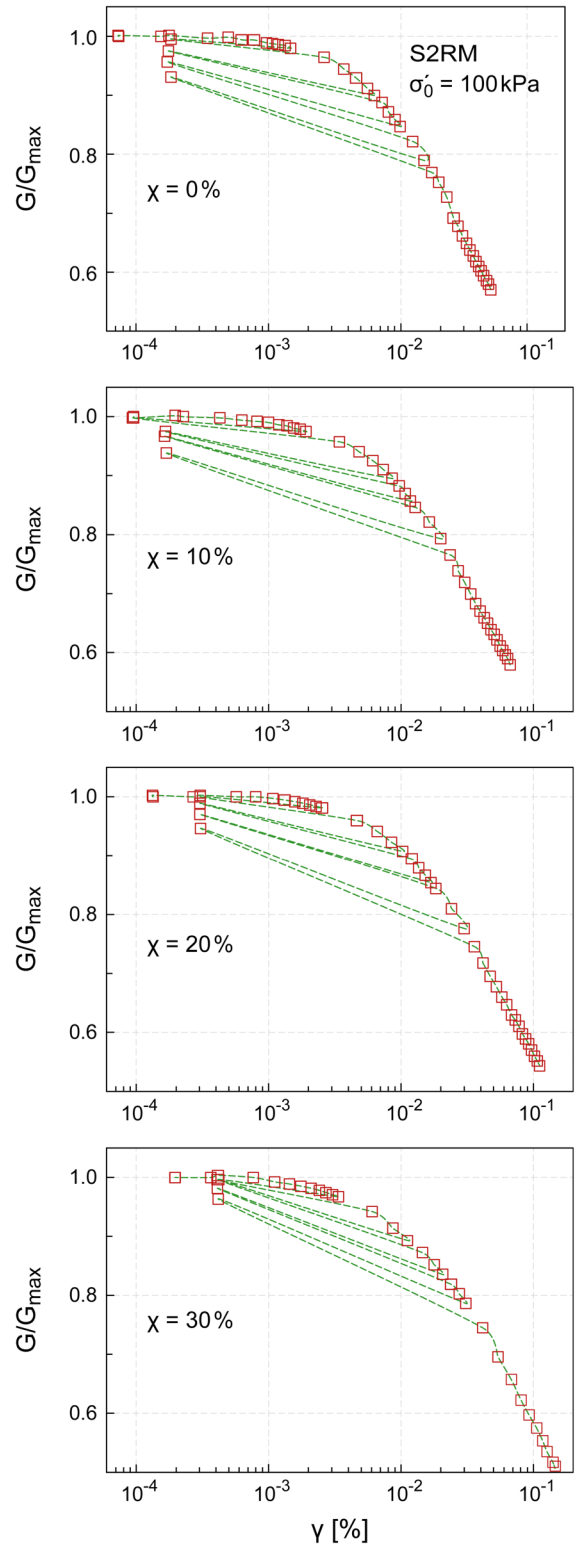

Fig. 13 Shear modulus reduction vs. shear strain during loading–unloading-reloading cycles for mixture S2RM at various rubber chips contents and confining stress equal to 100 kPa

for elastic behaviour, several tests with a sequence of loading–unloading-reloading cycles were performed. Figure 13 displays typical results for S2RM at 0/10/20/30% chips contents at confining stress of 100 kPa. The dashed lines indicate the loading path. Four cycles of unloading–reloading have been induced at strains where $G(\gamma)/G_{max}$ amounted to approx. 0.97, 0.90, 0.85 and 0.80. G_{max} is the small-strain value during virgin loading. The curves show that loading up to $G/G_{max}=0.97$ yields after unloading a small-strain value of $G/G_{max} \approx 1$. Continuation of loading to higher strains and subsequent unloading reduces G_{max} to a value $G_{max,\delta}<G_{max}$ thus indicating a permanent texture change. In other words, the soil particles are rearranged into a different structural framework to resist the load. As the rubber content increases, the degradation of the small strain stiffness becomes weaker. It is also interesting to note that upon re-loading the specimen returns to the same modulus on the "backbone" curve of the initial loading path, i.e. the form of the G/G_{max} versus γ curve is not altered by the unloading–reloading cycles. Comparisons among the three sands S2, S3 and S4 are displayed in Fig. 14 which shows the degradation of the small-strain value ($1-G_{max,\delta}/G_{max}$) against ($1- G/G_{max}$) at the distinct unloading cycles dependent on the rubber chips content. It can be clearly seen that sand S3 is the most susceptible among the three sands.

On the contrary, small-strain damping remains largely unaffected by preceding higher strain loading, at least up to strains corresponding to $G/G_{max}=0.8$. This has been observed for all sand-rubber mixtures.

As for the threshold strain for elastic, fully recoverable behaviour, an accurate determination was not possible from the specific test series, as they have not been designed for this purpose. Since all specimens did not exhibit any appreciable degradation up to at least $G/G_{max}=0.97$, the respective shear strain could be adopted as a first approximation for that threshold. For S2RM at 0/10/20/30% chips content and confining stress of 100 kPa observed values amounted to $1.47\cdot10^{-3}/1.92\cdot10^{-3}/2.54\cdot10^{-3}/3.34\cdot10^{-3}$%, respectively. At 30% chips content, strains even up to $1.1\cdot10^{-2}$% did not alter the specimen. The data clearly show that increasing the rubber chips content leads to an

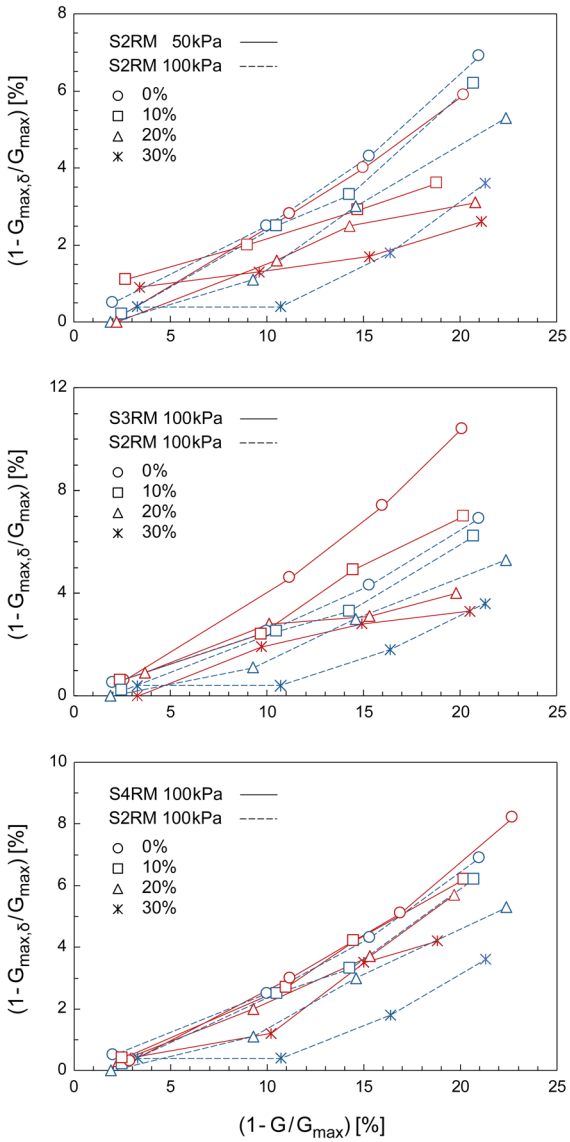

Fig. 14 Shear modulus degradation at the four distinct unloading–reloading cycles for the three mixtures at various rubber chips contents and confining stresses

increase in the threshold shear strain for recoverable behaviour. The same trend is observed for S3RM and S4RM, and at the other confining stresses.

4 Conclusions

The dynamic behaviour of sand rubber mixtures was evaluated through resonant column testing. Specimens of 100 mm in diameter and 200 mm high were prepared by mixing different sands with irregularly shaped, coarse rubber chips at rubber contents up to 30% by dry mass. All specimens were prepared at a relative density of 0.5 and tested under confining stress varying from 50 to 400 kPa. Both small and intermediate strain responses were measured.

At small strains, increasing the confining stress results in an increase of the shear modulus and a decrease of the damping ratio. Increasing the rubber content leads to a reduction of the shear modulus and to an increase of the damping ratio of the mixtures. For contents larger or equal to 20% the data points at all sands exhibit only minor differences.

At higher strains, increasing the confining stress flattens the curves of the shear modulus reduction and the increase of the damping ratio to higher strains. Adding more rubber has the same effect regarding the shear modulus. For the damping ratio, increasing the rubber content has an appreciable effect on the small strain value, which fades away at higher strains.

For the mixtures with chips content less than 20%, the overall response is controlled by the sand portion of the mixture while for a content equal to 20% and 30% the dynamic response is controlled both by sand and rubber particles.

A sequence of loading–unloading-reloading cycles at specific percentages of the small-strain shear modulus aimed at assessing the degradation of the material, i.e. the threshold beyond which a permanent texture change occurs. The results indicate that the composite material becomes more resistant as more rubber is added to the mixture.

The predictive equations derived from the data sets may be utilized to calculate the small strain values and also to assess the shear modulus reduction at higher strains, as for example needed in seismic site response analyses. Of course, these equations are valid only for the specific sands and rubber chips, as the characteristics of the rubber and the sand can be very different in terms of hardness, or particle shape.

Funding Open Access funding enabled and organized by Projekt DEAL. The authors have not disclosed any funding.

Data Availability Enquiries about data availability should be directed to the authors.

Declarations

Conflict of interest The authors have not disclosed any competing interests.

Open Access This article is licensed under a Creative Commons Attribution 4.0 International License, which permits use, sharing, adaptation, distribution and reproduction in any medium or format, as long as you give appropriate credit to the original author(s) and the source, provide a link to the Creative Commons licence, and indicate if changes were made. The images or other third party material in this article are included in the article's Creative Commons licence, unless indicated otherwise in a credit line to the material. If material is not included in the article's Creative Commons licence and your intended use is not permitted by statutory regulation or exceeds the permitted use, you will need to obtain permission directly from the copyright holder. To view a copy of this licence, visit http://creativecommons.org/licenses/by/4.0/.

References

Amuthan MS, Boominathan A, Banerjee S (2020) Undrained cyclic responses of granulated rubber-sand mixtures. Soil Found 60(4):871–885. https://doi.org/10.1016/j.sandf.2020.06.007

Anastasiadis A, Senetakis K, Pitilakis K (2012) Small-strain shear modulus and damping ratio of sand-rubber and gravel-rubber mixtures. Geotech Geol Eng 30:363–382. https://doi.org/10.1007/s10706-011-9473-2

ASTM D4015-15e1 (2015) Standard test methods for modulus and damping of soils by fixed-base resonant column devices. ASTM International, West Conshohocken, PA

Bahadori H, Farzalizadeh R (2018) Dynamic properties of saturated sand mixed with tyre powders and tyre shreds. Int J Civ Eng 16(4):395–408. https://doi.org/10.1007/s40999-016-0136-9

Banzibaganye G, Becker A, Vrettos C (2019) Static and cyclic triaxial tests on medium sand and tire chips mixtures. In: Proceedings of the 17th African Regional Conference on Soil Mechanics and Geotechnical Engineering, Cape Town, pp 163–168

Banzibaganye G (2022) Static and dynamic behaviour of sand-rubber chips mixtures. Doctoral Dissertation, Technical University of Kaiserslautern. https://doi.org/10.26204/kluedo/6749

Banzibaganye G, Vrettos C (2022) Sand tyre chips mixtures in undrained and drained cyclic triaxial tests. Proc Inst Civ Eng: Ground Improv 175(1):23–33. https://doi.org/10.1680/jgrim.20.00046

Becker A, Vrettos C (2011) Bodenmechanische Untersuchungen an Mischungen von rolligen und bindigen Böden mit Gummi aus Recyclingprozessen. Bauingenieur 87:548–556

Bernal-Sanchez J, McDougall J, Barreto D, Marinelli A, Dimitriadi V, Anbazhagan P, Miranda M (2019) Experimental assessment of stiffness and damping in rubber-sand mixtures at various strain levels. In: Silvestri F, Moraci N (eds) Earthquake geotechnical engineering for protection and development of environment and constructions. CRC Press, London, pp 1403–1410

Das S, Bhowmik D (2020) Dynamic behaviour of sand–crumbed rubber mixture at low strain level. Geotech Geol Eng 38:6611–6622. https://doi.org/10.1007/s10706-020-01458-4

Ehsani M, Shariatmadari N, Mirhosseini SM (2015) Shear modulus and damping ratio of sand-granulated rubber mixtures. J Cent South Univ 22:3159–3167. https://doi.org/10.1007/s11771-015-2853-7

Feng Z-Y, Sutter KG (2000) Dynamic properties of granulated rubber/sand mixtures. Geotech Test J 23(3):338–344. https://doi.org/10.1520/GTJ11055J

Fonseca J, Riaz A, Bernal-Sanchez J, Barreto D, McDougall J, Miranda-Manzanares M, Marinelli A, Dimitriadi V (2019) Particle-scale interactions and energy dissipation mechanisms in sand-rubber mixtures. Geotech Lett 9:1–6. https://doi.org/10.1680/jgele.18.00221

Foose GJ, Benson CH, Bosscher PJ (1996) Sand reinforced with shredded waste tires. J Geotech Eng 122(9):760–767. https://doi.org/10.1061/(ASCE)0733-9410(1996)122:9(760)

Hazarika H, Pasha SMK, Ishibashi I, Yoshimoto N, Kinoshita T, Endo S, Karmokar AK, Hitosugi T (2020) Tire-chip reinforced foundation as liquefaction countermeasure for residential buildings. Soils Found 60(2):315–326. https://doi.org/10.1016/j.sandf.2019.12.013

GDS Instruments (2015) GDS resonant column: the GDS resonant column system handbook. Hook, U.K

Kaneko T, Orense RP, Hyodo M, Yoshimoto N (2013) Seismic response characteristics of saturated sand deposits mixed with tire chips. J Geotech Geoenviron Eng 139(4):633–643. https://doi.org/10.1061/(ASCE)GT.1943-5606.0000752

Li B, Huang M, Zeng X (2016) Dynamic behaviour and liquefaction analysis of recycled-rubber sand mixtures. J Mater Civ Eng 28(11):04016122. https://doi.org/10.1061/(ASCE)MT.1943-5533.0001629

Madhusudhan BR, Boominathan A, Banerjee S (2018) Comparison of cyclic triaxial test results on sand–rubber tire shred mixtures with dynamic simple shear test results. Geotech Earthq Eng Soil Dyn. https://doi.org/10.1061/9780784481486014

Madhusudhan BR, Boominathan A, Banerjee S (2020) Cyclic simple shear response of sand–rubber tyre chip mixtures. Int J Geomech 20(9):04020136. https://doi.org/10.1061/(ASCE)GM.1943-5622.0001761

Mashiri MS, Vinod JS, Sheikh MN (2016) Liquefaction potential and dynamic properties of sand-tyre chip (STCh) mixtures. Geotech Test J 39(1):69–79. https://doi.org/10.1520/GTJ20150031

Nakhaei A, Marandi S, Kermani S, Bagheripour M (2012) Dynamic properties of granular soils mixed with granulated rubber. Soil Dyn Earthq Eng 43:124–132. https://doi.org/10.1016/j.soildyn.2012.07.026

Pistolas GA, Anastasiadis A, Pitilakis K (2018) Dynamic behaviour of granular soil materials mixed with granulated rubber: effect of rubber content and granularity on the small-strain shear modulus and damping ratio. Geotech Geol Eng 36:1267–1281. https://doi.org/10.1007/s10706-017-0391-9

Pitilakis D, Anastasiadis A, Vratsikidis A, Kapouniaris A, Massimino MR, Abate G, Corsico S (2021) Large-scale field testing of geotechnical seismic isolation of structures using gravel-rubber mixtures. Earthq Eng Struct Dyn 50:2712–2731. https://doi.org/10.1002/eqe.3468

Rios S, Kowalska M, Viana da Fonseca A (2021) Cyclic and dynamic behavior of sand–rubber and clay–rubber mixtures. Geotech Geol Eng 39:3449–3467. https://doi.org/10.1007/s10706-021-01704-3

Senetakis K, Anastasiadis A, Pitilakis K, Souli A (2011) Dynamic behavior of sand/rubber mixtures. Part II: effect of rubber content on G/Go-γ-DT curves and volumetric threshold strain. J ASTM Int 9(2):1–12. https://doi.org/10.1520/JAI103711

Senetakis K, Anastasiadis A, Pitilakis K (2012) Dynamic properties of dry sand/rubber (SRM) and gravel/rubber (GRM) mixtures in a wide range of shearing strain amplitudes. Soil Dyn Earthq Eng 33(1):38–53. https://doi.org/10.1016/j.soildyn.2011.10.003

Vrettos C, Savidis S (1999) Shear modulus and damping for Mediterranean clays of medium plasticity. In: Seco e Pinto P (eds) Earthquake geotechnical engineering: Proceedings of the second international conference on earthquake geotechnical engineering. A.A. Balkema, Rotterdam, vol 1, pp 71–76

Vrettos C, Banzibaganye G (2022) Effects of specimen size and inertia on resonant column tests applied to sands. Soil Dyn Earthq Eng 155:107136. https://doi.org/10.1016/j.soildyn.2021.107136

Zornberg JG, Cabral AR, Viratjandr C (2004) Behaviour of tire shred-sand mixtures. Can Geotech J 41(2):227–241. https://doi.org/10.1139/t03-086

Publisher's Note Springer Nature remains neutral with regard to jurisdictional claims in published maps and institutional affiliations.